Targeting the adenosinergic system: Ligand binding kinetics and label-free assays for the study of SLC29A1 transporter and A2B adenosine receptor

Vlachodimou A.

CHAPTER 3

Kinetic profiling and functional characterization of 8-phenylxanthine derivatives as A_{2B} adenosine receptor antagonists

Anna Vlachodimou, Henk de Vries, Milena Pasolli, Miranda Goudswaard, Soon-Ae Kim, Yong-Chul Kim, Mirko Scortichini, Laura H. Heitman, Kenneth A. Jacobson, and Adriaan P. IJzerman

Manuscript in preparation

Abstract

A_{2B} adenosine receptor antagonists have therapeutic potential in inflammation-related diseases such as asthma, chronic obstructive pulmonary disease and cancer. However, no drug is currently clinically approved, creating a demand for research on novel antagonists. Over the last decade, the study of target binding kinetics, along with affinity and potency, has been proven valuable in early drug discovery stages, as it is associated with improved *in vivo* drug efficacy and safety. In this study, we report the synthesis and biological evaluation of a series of xanthine derivatives as antagonists of the A_{2B}AR. All compounds were assessed in radioligand binding experiments, to evaluate their affinity and kinetic binding parameters. Both structure-affinity and structure-kinetic relationships were derived. Among 27 compounds tested, two structurally similar compounds, **17** and **18**, were further evaluated in a label-free assay due to their divergent kinetic profiles. An extended cellular response was associated with a long A_{2B}AR residence time. This link between a ligand's residence time on the A_{2B}AR and its functional effect highlights the importance of binding kinetics as a selection parameter in the early stages of drug discovery.

Introduction

The A_{2B} adenosine receptor (A_{2B}AR) belongs to the superfamily of rhodopsin-like G protein-coupled receptors (GPCRs), being a member of the adenosine receptor (AR) family. It has been mapped on chromosome 17p11.2-12 and as all GPCRs the encoded protein consists of a seven transmembrane α-helix architecture[1, 2]. Adenosine, a ubiquitous purine nucleoside, is the endogenous ligand for all ARs, *i.e.* A_1, A_{2A}, A_{2B} and A_3. These AR subtypes are coupled to different effectors and control different physiological and pathophysiological conditions. A_{2B}AR is the least well characterized of the four AR subtypes, possibly due to its low affinity for adenosine[3]. Under physiological conditions A_{2B}AR is considered to remain silent, as the extracellular concentration of adenosine ranges from 20 to 300 nM, much lower than the reported half maximal effective concentration (EC_{50}) of adenosine for A_{2B}AR (EC_{50} = 24 μM)[4, 5]. In contrast, under pathophysiological conditions extracellular concentrations of adenosine could rise up to 30 μM, therefore resulting in A_{2B}AR activation and signaling.

A_{2B}ARs are present in numerous tissues and organs, including bowel, bladder, lung, brain, as well as on hematopoietic and mast cells[2, 6]. Interestingly, A_{2B}AR expression levels are often (up)regulated during disease. The high expression of the receptor in conjunction with the increased extracellular adenosine concentration under pathophysiological conditions render A_{2B}AR antagonists interesting pharmacological and therapeutic tools for a broad spectrum of diseases, such as asthma, chronic obstructive pulmonary disease [7, 8], colon inflammation[9, 10], diabetes[11] and cancer[12]. Adenosine production is upregulated in the tumor microenvironment and acts at both A_{2A}AR and A_{2B}AR to facilitate tumor progression *in vivo*[13]. In cancer models, A_{2B}AR antagonists impede adenosine-induced tumor cell proliferation, angiogenesis and metastasis, and remove immune suppression[14].

Over the past years, several xanthine and non-xanthine derivatives have been synthesized and evaluated for their A_{2B}AR affinity and selectivity[15]. However, no A_{2B}AR-selective antagonist has reached the market yet for therapeutic use. Only CVT-6883 has completed Phase I clinical trials with no adverse events reported, while another clinical trial for PBF-1129, as drug candidate for locally advanced or metastatic non-small cell lung carcinoma, is under recruitment[16, 17].

The 3D structure of A_{2B}AR has not been elucidated yet, hence, the design of new potential drug candidates is mainly based on more classical structure-affinity relationships[18]. Although affinity is a key parameter in pharmacology, it does not necessarily predict *in vivo* efficacy. The last decade an increasing number of studies suggested that the study of ligand binding kinetics, quantified by association (k_{on}) and dissociation (k_{off}) rate constants, is highly relevant in the early stages of drug discovery, as *in vivo* efficacy is linked to optimized kinetic characteristics in many cases[19]. A typical example is the neurokinin 1 (NK_1) receptor antagonist aprepitant. Aprepitant has been found to have higher *in vivo* efficacy than other NK_1 receptor antagonists with similar thermodynamic affinities, due to its long residence time (RT:

$1/k_{off}$) at the NK_1 receptor[20].

Here, we report on the synthesis of a number of xanthine-based A_{2B}AR antagonists, on the affinities of these and a number of previously reported xanthines, and on their target binding kinetic parameters obtained in radioligand binding assays. We show that most xanthine derivatives present high affinity for A_{2B}AR, while displaying a variety in association and dissociation rate constants. Additionally, we developed a label-free impedance-based assay using intact cells expressing A_{2B}AR for the further characterization of compounds with diverse kinetic profiles. Compounds **17** and **18** showing a long and short RT on the receptor, respectively, were profiled in this assay. Compound **17**, with the longer RT, had a more sustained effect than compound **18**.

Results and Discussion

CHEMISTRY.

2-(4-(2,6-Dioxo-1,3-dipropyl-2,3,6,7-tetrahydro-1H-purin-8-yl)phenoxy)acetic acid (xanthine carboxylic congener, XCC, 1) was synthesized as reported[21]. Its amide derivatives **3**-**7**, **9**, **10**, **20**-**25** were prepared by reaction with the desired amine in the presence of EDAC and DMAP as carboxyl group activating agents (Scheme 1).

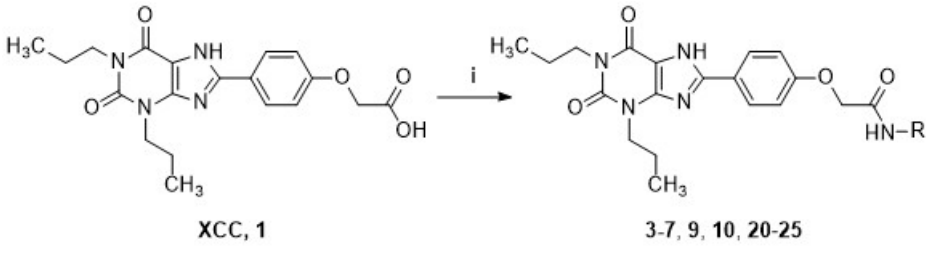

XCC, 1 3-7, 9, 10, 20-25

Reagents and conditions: i. EDAC, DMAP, primary or secondary amine, DMF, rt, 18h

Scheme 1: Synthesis of XCC amides.

BIOLOGICAL EVALUATION.

Validation of [^{3}H]PSB 603 equilibrium and kinetic radioligand binding assays

Firstly, the tritium-labeled A_{2B}AR antagonist 8-[4-[4-(4-chlorophenzyl)piperazide-1-sulfonyl) phenyl]]-1-propylxanthine ([^{3}H]PSB 603) was characterized on CHO-spap-hA_{2B} membranes. In a saturation binding assay receptor binding was saturable and quantified by a K_D value of 1.71 nM and a B_{max} value of 4.30 pmol/mg (Figure 1A, Table 1). The K_D value is comparable with the value previously reported by Bormann *et al.*[22]. When evaluated in homologous displacement assay, unlabeled PSB 603 showed similar affinity, yielding a pK_i value of 8.90 (Figure 1D, Table 1).

Subsequently, [^{3}H]PSB 603 was evaluated in kinetic binding assays in order to determine its kinetic binding parameters k_{on} and k_{off} (Figure 1B, Table 1). [^{3}H]PSB 603 associated rapidly to the hA$_{2B}$AR and equilibrium binding was reached within 20 min, while complete dissociation was reached within 55 min, resulting in a k_{off} value of 0.075 min^{-1}. The association and dissociation experiments resulted in the calculation of k_{on} and RT values of 0.096 nM^{-1} min^{-1} and 13 min, respectively. Based on the kinetic data a dissociation constant (kinetic K_D) was calculated to be 0.78 nM, hence it is in good agreement with the affinity determined by equilibrium saturation binding and displacement experiments, as well as with the available literature data[22].

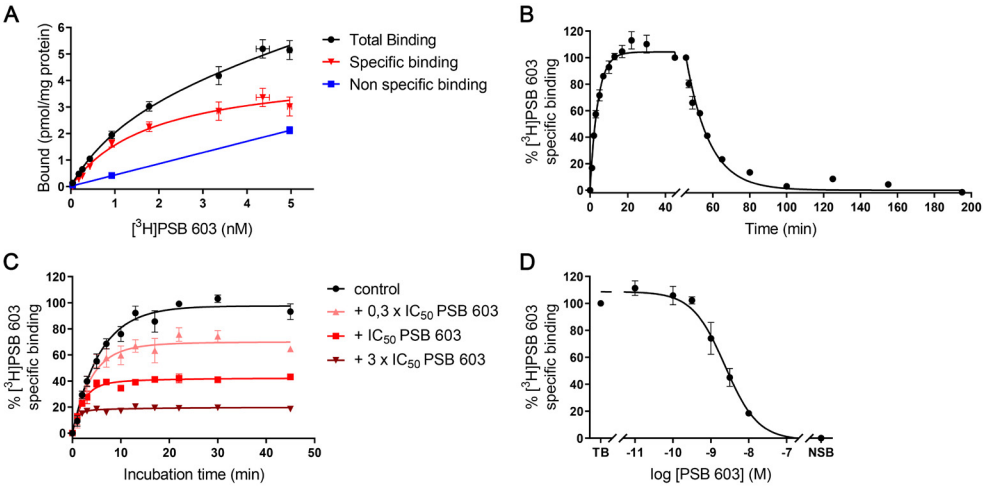

Figure 1: Characterization of [^{3}H]PSB 603 binding to hA$_{2B}$AR expressed on CHO-spap-hA$_{2B}$AR membranes at 25 °C. (A) Binding of [^{3}H]PSB 603 in an equilibrium saturation assay. (B) Association and dissociation kinetics of 1.5 nM [^{3}H]PSB 603 to and from hA$_{2B}$AR. (C) Competition association assay of [^{3}H]PSB 603 in the absence or presence of 0.3x, 1x, and 3x IC$_{50}$ of unlabeled PSB 603. (D) Homologous displacement of [^{3}H]PSB 603 from hA$_{2B}$AR. Data are shown as mean ± SEM from at least three independent experiments performed in duplicate.

To obtain kinetic binding parameters for unlabeled A$_{2B}$AR antagonists, a radioligand competition association assay was developed. This Motulsky-Mahan model-based assay determines the time-dependent binding of two competing ligands[23] and has been used to investigate the binding kinetics of ligands for various targets, such as GPCRs[24, 25], kinases[26], transporters[27, 28] and other proteins[29]. The specific binding of [^{3}H]PSB 603 was measured in the absence and presence of unlabeled PSB 603 over a time course of 45 min (Figure 1C) and k_{on}, k_{off} and kinetic K_D values of unlabeled PSB 603 were calculated to be 0.109 nM^{-1} min^{-1}, 0.084 min^{-1} and 0.77 nM, respectively (Table 1). As the values of the competition association assay were in excellent agreement with the ones from the association and dissociation assay

(Table 1), the first was deemed validated for determining unlabeled ligand's binding kinetics.

In order to increase the throughput of the assay, a single concentration of PSB 603 (1.0-fold its IC_{50}) was tested. Association and dissociation rate constants were found to be similar to the aforementioned ones, *i.e.* 0.111 ± 0.014 nM^{-1} min^{-1} and 0.086 ± 0.007 min^{-1} for k_{on} and k_{off} respectively (data not shown). Consequently, all other compounds were tested only at one concentration equal to 1.0-fold their IC_{50} determined from displacement experiments.

Determination of equilibrium binding affinity (K_i) of A_{2B}AR antagonists

Once the necessary tool assays were developed and validated, various xanthine-based A_{2B}AR antagonists were examined. The affinities of all 29 compounds were evaluated in an equilibrium radioligand displacement study using [^{3}H]PSB 603 as the radiolabeled competitor. All compounds fully displaced the radioligand from the hA_{2B} receptor in a concentration-dependent manner. The data were fitted in a one-phase competition model showing mono-phasic displacement. A wide spread of affinities was noticed, ranging from 61.4 μM for compound **4** to 1.78 nM for compound **13**; all affinities are listed in Tables 2-4.

Evaluation of kinetic binding parameters (k_{on}, k_{off}, RT) of A_{2B}AR antagonists

Any compound with a K_i value <100 nM was assessed in kinetic binding assays, *i.e.* competition association assay. All kinetic data are listed in Tables 2-4. The k_{on} values of the 17 tested compounds exhibited a 26-fold range, spanning from 0.0014 nM^{-1} min^{-1} for **14** to 0.036 nM^{-1} min^{-1} for **3**. To the contrary, k_{off} values displayed a greater 94-fold variation, with compounds **17** and **3** defining the lower and upper limits, *i.e.* 0.011 min^{-1} and 1.071 min^{-1}, respectively. In Figure 2A the curves of a long (**17**) and short (**18**) RT compound are presented over a time course of 3 hr. The overshoot followed by a steady decrease to a lower equilibrium is characteristic of a long RT compound, while a compound with a shorter RT than the radioligand presents a curve with a shallower ascension till equilibrium is reached.

Evaluation and incorporation of target binding kinetics has been found to be a crucial parameter in drug optimization. The association rate constant is crucial for high target occupancy, due to the resulting rebinding effect[30], as well as for drug selectivity over different targets and ultimately for increased drug safety[31]. Last but not least, a fast association is crucial for an immediate drug response in case of an acute pathological event[32, 33]. As far as the dissociation rate constant is concerned, a slow rate, hence a long RT is required for a longer effect[34]. Assuming that the RT exceeds the pharmacokinetic half-life, the drug could maintain its effect even past plasma clearance, resulting in potential advantages like a decreased frequency of drug dosing and a reduction in off-target toxic effects[35, 36].

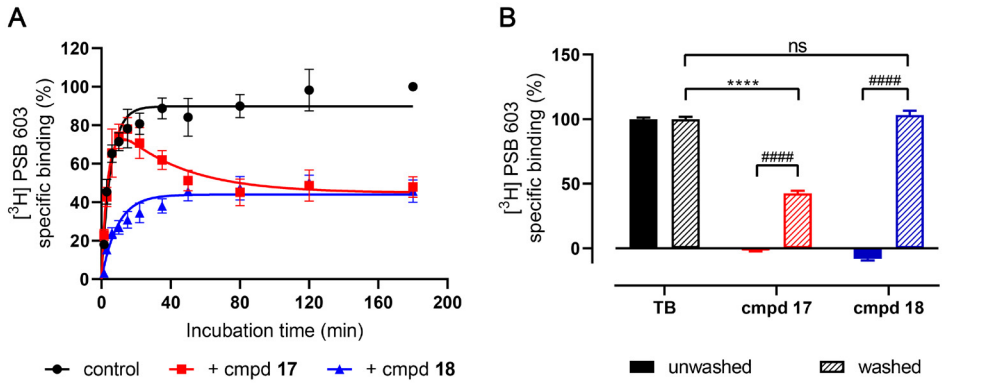

Figure 2: Evaluation of the binding kinetics of compounds **17** and **18** at 25 °C. (A) Competition association experiment of specific [^{3}H]PSB 603 binding to A_{2B}AR on CHO-spap-hA_{2B}AR membranes (25°C) in the absence or presence of an IC_{50} concentration of a longer (**17**) and shorter (**18**) RT compound compared to control. (B) Recovery of radioligand binding after washing. Compound binding at 10xIC_{50} concentration after no (unwashed) and 3x (washed) washing. Data are shown as mean ± SEM from at least three independent experiments performed in duplicate. The results of both washed and unwashed samples were compared to the control condition (TB) without any competitor (100% washed and unwashed radioligand binding, respectively). #### $P \leq 0.0001$ determined in an unpaired t-test with Welch's correction. ns $P > 0.05$, **** $P \leq 0.0001$ determined in a one-way ANOVA test with Dunnett's correction.

Evaluation of ligand binding recovery with a washout assay

To validate the results of the competition association assay and distinguish between ligands with distinct kinetic binding parameters, a [^{3}H]PSB 603 washout assay was developed (Figure 2B, Table 5). Compounds **18** and **17** were selected as they present a short (8 min) and long (87 min) RT compound, respectively, while they have similar structures and affinities.

Both the washed and the unwashed conditions were assessed. For the washed condition, the unlabeled compounds were incubated with the target for 2 hr, followed by three wash and centrifugation cycles. Subsequently, [^{3}H]PSB 603 was co-incubated which led to competition of the radioligand with the unlabeled ligand still bound after the washing procedure. For the unwashed condition no washing was performed before the determination of radioligand displacement. Based on the experimental set-up, the long RT compound would be predicted to remain bound to A_{2B}ARs, as it would not be removed during the washing steps, and thus to result in lower radioligand binding.

In the unwashed condition, all A_{2B}ARs were fully occupied by each of the compounds as there was no specific binding of [^{3}H]PSB 603 observed (Figure 2B; unwashed). When the washed and unwashed conditions for both compounds **17** and **18** (Figure 2B; washed and unwashed) were compared, a significant increase in

radioligand binding after washing was monitored, indicating that they had (partially) dissociated from the target and been washed away. In the washed condition, the recovery of [^{3}H]PSB 603 binding was increased proportional to the duration of binding of the compound to the target. The short RT compound **18** did not show any significant difference ($P > 0.05$; Figure 2B, washed) in specific [^{3}H]PSB 603 binding compared to control (TB). Apparently, **18** was completely removed during the washing procedure. On the other hand, the long RT compound **17** was washed away for 58%, indicating that 42% of A_{2B}ARs were still occupied by this ligand after the applied washing cycles, showing a significant ($P < 0.0001$, Figure 2B, washed) decrease of [^{3}H]PSB 603 specific binding compared to control (TB).

Structure-Affinity Relationships (SAR) and Structure-Kinetic Relationships (SKR).

Intrigued by earlier studies we explored a whole series of xanthine derivatives[37]. We started with the study of the prototypic A_{2B}AR antagonist MRS 1754 (**13**). In the displacement assay an affinity of 1.78 nM was determined, which was in excellent agreement with data reported by Ji *et. al.* [38]. The kinetic characterization of **13** made us increase the duration of the competition association assay from 45 min to 3 hr as its determined RT was 69 min. As a result the 3 hr incubation assay was used for the determination of kinetic binding parameters for all A_{2B}AR antagonists.

We initiated the investigation on the xanthine scaffold by compound **1**[21]. Its affinity was found to be higher than 100 nM, the limit set as threshold for the kinetic studies. By substitution of the acid moiety for an acetamide (**2**) the affinity increased approx. 7-fold. Therefore, this acetamide was incorporated in all other compounds synthesized and tested. For compound **2**, it was not possible to determine its kinetic characteristics, most probably because they were outside the detection range of our method.

Further functionalization of the acetamide to incorporate a cyclopropyl group (**3**) decreased the affinity, an effect observed for every non-aromatic ring tested (**3**, **4**, **5**, **7**). When pyrazole was incorporated (**6**) the affinity increased compared to compound **5**, but it remained in the micromolar range. To the contrary, introduction of pyridine (**9**) and pyrazine (**10**) decreased affinity even further when compared to the cyclohexyl substitution (**7**). Only incorporation of a phenyl ring (**8**) resulted in a low nanomolar affinity (1.93 nM) and a RT of 46 min. In addition to the cyclic substituents, a linear one (**11**) was incorporated, leading to a decrease in affinity compared to compound **2**. However, the affinity did not exceed the 100 nM threshold.

Table 1: Comparison of the affinity, dissociation constants and kinetic parameters of PSB 603, obtained with different radioligand binding assays performed on CHO-spap-hA_{2B}AR membranes.

Assay	B_{max} (pmol/mg)	K_D (nM)	pK_i (K_i (nM))	k_{on} (nM^{-1} min^{-1})	k_{off} (min^{-1})	RT (min)
Saturation binding	4.30 ± 0.30	1.71 ± 0.14	-	-	-	-
Displacement	-	-	8.90 ± 0.10 (1.25)	-	-	-
Association and dissociation	-	0.78 ± 0.09[a]	-	0.096 ± 0.010	0.075 ± 0.003	13 ± 0.6
Competition association	-	0.77 ± 0.10[a]	-	0.109 ± 0.008[b]	0.084 ± 0.009[b]	12 ± 1.3

Values are mean ± SEM of at least three individual experiments performed in duplicate. [a]Kinetic affinity values (K_D) determined by association and dissociation, and competition association assay, is defined as $K_D = k_{off}/k_{on}$. [b] Kinetic parameters of unlabeled PSB 603 were determined by addition of 0.3-, 1- and 3-fold its IC_{50} value.

Table 2: Affinity (pK_i) and Kinetic Parameters (k_{on}, k_{off}, RT) of hA_{2B}AR antagonists **1** – **11**.

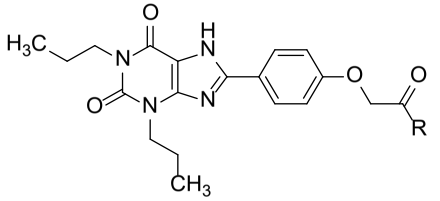

cmpd	R	pK_i (K_i (nM))	k_{on} (nM^{-1} min^{-1})	k_{off} (min^{-1})	RT[a] (min)
1	OH	6.78 ± 0.06 (167)	n.d.[b]	n.d.	n.d.
2	NH_2	7.60 ± 0.07 (25.1)	Kinetics outside the range of the assay (see text)		

3	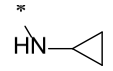	7.44 ± 0.09 (36.3)	0.036 ± 0.006	1.071 ± 0.027	0.9 ± 0.0
4	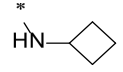	4.21 ± 0.14 (61423)	n.d.	n.d.	n.d.
5	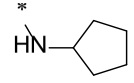	4.78 ± 0.17 (16749)	n.d.	n.d.	n.d.
6	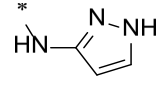	5.26 ± 0.05 (5483)	n.d.	n.d.	n.d.
7	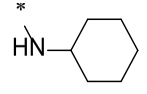	6.02 ± 0.09 (951)	n.d.	n.d.	n.d.
8	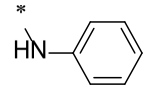	8.71 ± 0.01 (1.93)	0.015 ± 0.000	0.022 ± 0.006	46 ± 13
9	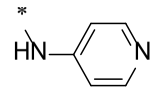	5.87 ± 0.16 (1351)	n.d.	n.d.	n.d.
10	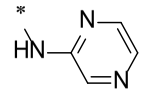	5.16 ± 0.08 (6950)	n.d.	n.d.	n.d.
11	$N(CH_3COOEt)_2$	6.95 ± 0.00 (113)	n.d.	n.d.	n.d.

Values represent the mean ± SEM of at least three individual experiments, performed in duplicate. [a]RT =1/k_{off} [b]n.d. = not defined

Table 3: Affinity (pK_i) and Kinetic Parameters (k_{on}, k_{off}, RT) of $hA_{2B}AR$ antagonists **12** – **18**.

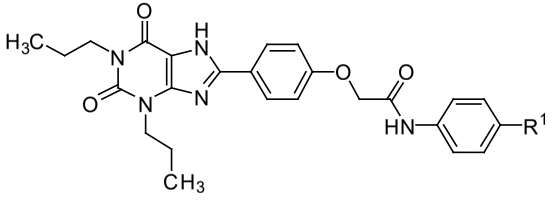

cmpd	R^1	pKi (Ki (nM))	k_{on} (nM^{-1} min^{-1})	k_{off} (min^{-1})	RT[a] (min)	K_D[b] (nM)
12	CH_3	8.47 ± 0.06 (3.42)	0.007 ± 0.002	0.018 ± 0.008	55 ± 25	2.7 ± 1.5
13	CN	8.75 ± 0.20 (1.78)	0.024 ± 0.005	0.015 ± 0.001	69 ± 2.4	0.61 ± 0.14
14	NO_2	7.87 ± 0.04 (13.5)	0.0014 ± 0.0003	0.017 ± 0.006	58 ± 19	12 ± 4.9
15	CF_3	8.54 ± 0.06 (2.86)	Kinetics outside the range of the assay (see text)			
16	$COCH_3$	8.52 ± 0.05 (3.03)	0.011 ± 0.001	0.019 ± 0.006	54 ± 18	1.7 ± 0.58
17	$COOCH_3$	8.64 ± 0.05 (2.29)	0.006 ± 0.001	0.011 ± 0.004	87 ± 29	1.8 ± 0.62
18	$CONHCH_3$	7.70 ± 0.06 (19.9)	0.012 ± 0.001	0.125 ± 0.003	8.0 ± 0.2	10 ± 0.89

Values represent the mean ± SEM of at least three individual experiments, performed in duplicate. [a]$RT = 1/k_{off}$. [b]Kinetic K_D values, defined as $K_D = k_{off}/k_{on}$.

Table 4: Affinity (pK_i) and Kinetic Parameters (k_{on}, k_{off}, RT) of $hA_{2B}AR$ antagonists **19** – **27**.

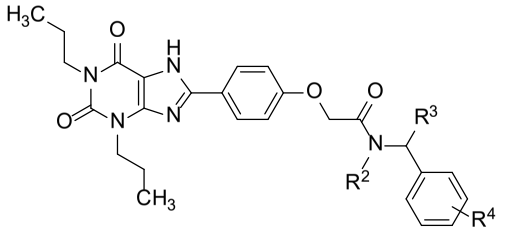

cmpd	R^2	R^3	R^4	pK_i (K_i (nM))	k_{on} (nM^{-1} min^{-1})	k_{off} (min^{-1})	RT[a] (min)	K_D[b] (nM)
19	H	H	H	6.15 ± 0.15 (711)	n.d.[c]	n.d.	n.d.	n.d.
20	H	H	4-CH_3	8.04 ± 0.04 (9.08)	0.004 ± 0.0015	0.046 ± 0.007	22 ± 3.5	12 ± 4.7
21	H	H	4-F	8.44 ± 0.06 (3.60)	0.017 ± 0.007	0.066 ± 0.015	15 ± 3.5	3.8 ± 1.7
22	H	H	4-Br	8.24 ± 0.11 (5.73)	0.007 ± 0.002	0.043 ± 0.019	23 ± 11	6.5 ± 3.6
23	H	H	3,4-diOH	7.61 ± 0.04 (24.4)	0.004 ± 0.001	0.099 ± 0.011	10 ± 1.1	27 ± 7.9
24	H	CH_3	H	7.82 ± 0.07 (15.2)	0.022 ± 0.008	0.164 ± 0.042	6.1 ± 1.6	7.5 ± 3.9
25	H	CH_3	H	8.09 ± 0.04 (8.11)	0.011 ± 0.003	0.097 ± 0.021	10 ± 2.3	8.6 ± 3.0
26	H		H	7.42 ± 0.18 (37.9)	0.0017 ± 0.0006	0.053 ± 0.017	19 ± 6.2	31 ± 16
27	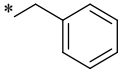	H	H	6.92 ± 0.05 (119)	n.d.	n.d.	n.d.	n.d.

Values represent the mean ± SEM of at least three individual experiments, performed in duplicate. [a]RT =1/k_{off}. [b]Kinetic K_D values, defined as K_D= k_{off}/k_{on}. [c]n.d. = not defined

Taking these results into consideration we continued with *para* substitution of the phenyl ring and determined the influence of those substituents on affinity and kinetic binding parameters. When we substituted compound **8** with a p-methyl group (**12**) a slight decrease in affinity and a 10 min increase in RT were observed. Introduction of a p-cyano group (**13**) increased RT further, while the association rate constant increased about 4 times, yielding a compound with subnanomolar affinity. The introduction of other electron withdrawing groups at the p-position (**14**, **15**, **16**, **17**, **18**) also yielded high affinity values for the receptor. Introduction of a nitro (**14**) or methyl ketone (**16**) substituent resulted in a moderate RT of 58 and 54 min, respectively, while the k_{on} value was largely varying, with **14** presenting a slow association to the receptor. The trifluoromethyl substituent (**15**) resulted in a high affinity for the receptor, while its kinetic characteristics could not be monitored due to the detection range of the assay. Introduction of a carboxylic acid (**17**) was responsible for the longest RT measured in this study, while a methylcarboxamide (**18**) resulted in a similar affinity but significantly shorter RT.

Subsequently, the introduction of a spacer between the acetamide and the phenyl ring was investigated (Table 4). By introducing a carbon linker (**19**) to compound **8**, the affinity dropped to a value in the micromolar range. A similar trend was observed for compounds **12** and **20**. Although affinity was decreased by 3-fold, it still remained in the nanomolar range for both compounds (**12** and **20**) allowing their kinetic characterization. The k_{on} value slightly decreased (0.007 nM^{-1} min^{-1} and 0.004 nM^{-1} min^{-1} for **12** and **20**, respectively), while RT was lessened by about 3-fold for **20**. Substitution of methyl (**20**) by fluoro (**21**), bromo (**22**) and di-hydroxy (**23**) did not lead to significant alteration of affinity, while RT remained to be 20 min or less. Only **21** yielded an increased k_{on} value, hence a faster association to $hA_{2B}AR$. Furthermore, the linker was altered by a methyl substitution on the R^2 position. The two enantiomers, R (**24**) and S (**25**), exhibited similar affinities and kinetic characteristics, with **24** showing approx. 2-fold increased k_{on} and k_{off} values compared to **25**, although the RT was short in both cases. When a phenyl ring was introduced on the R^2 position (**26**), the affinity slightly dropped compared to **24** and **25**, which after kinetic analysis appeared due to a decrease in association rate constant.

Finally, the benzyl substitution of the amido group (**27**) resulted in an increase in affinity compared to the unsubstituted **19**, indicating that this benzyl moiety is well accommodated in the binding pocket of $A_{2B}AR$. However, when compared to **26**, **27** showed a lower affinity, suggesting that **27** did not optimally fit.

Correlation plots

To obtain a better comparison of kinetic and affinity parameters and understand their relationship, correlation plots were constructed (Figure 3). The affinity obtained from traditional radioligand displacement assay (pK_i) and the kinetic affinity (pK_D) derived from the radioligand competition association assay were found to be

significantly correlated (r = 0.95, $P < 0.0001$; Figure 3A), validating the use of the competition association assay. When the association rate constants (log k_{on}) of all kinetically characterized compounds were plotted against the kinetic affinity (Figure 3B), a low, non-significant correlation was observed (r = 0.36, $P = 0.202$). However, the kinetic affinity was found to be significantly and strongly correlated with the dissociation rate constants (pk_{off}) (r = 0.76, $P = 0.0015$) (Figure 3C).

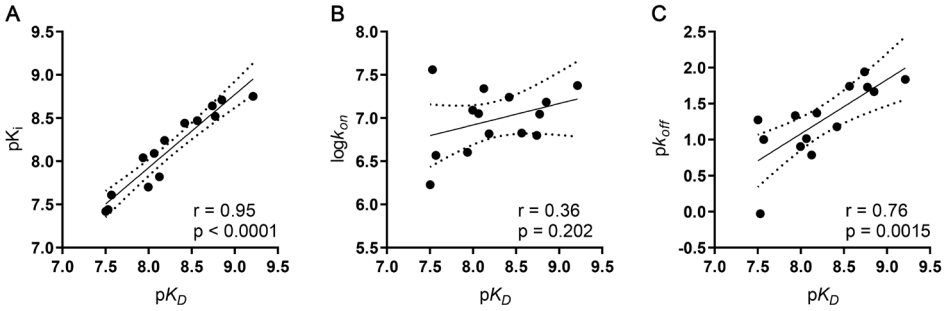

Figure 3: Correlation plots between affinity and kinetic parameters. Kinetic affinity (pK_D) is plotted against (A) affinity determined from typical displacement assays (pK_i); (B) association rate constant (logk_{on}); (C) dissociation rate constant (pk_{off}). The solid line corresponds to the linear regression of the data and the dotted lines represent the 95% confidence intervals for regression. Correlation was tested with Pearson r coefficient, while significance was shown with a *P* value. Data used in the plots are from Tables 2-4. Data are expressed as mean from at least three independent experiments performed in duplicate.

Functional characterization of compounds 17 and 18

Next to binding parameters we studied compounds **17** and **18** in a functional set-up, in order to investigate the link between binding kinetics and a possibly prolonged functional effect. For this purpose a label-free assay was developed, which is regarded as a translational step towards *in vivo* experiments[39]. The method was established with xCELLigence technology, measuring changes in cellular impedance that are expressed as a unitless parameter named Cell Index[40, 41].

Initials experiments with NECA (5'-N-ethylcarboxamidoadenosine), a non-selective AR agonist, were performed on control CHO-spap and CHO-spap-hA_{2B}ARs cells (Figure 4). No response was found on "empty" CHO-spap cells upon treatment with NECA, whereas a concentration-dependent response was measured on CHO-spap-hA_{2B}ARs cells, yielding a pEC_{50} value of 8.95 (Table 5). Although this seems to be a relatively high potency of NECA for A_{2B}AR[42, 43], it complies with other data in literature[44-47]. In order to validate that the response measured on CHO-spap-hA_{2B}ARs was only A_{2B}AR mediated, we pre-incubated cells with selective antagonists for each AR subtype prior to NECA stimulation. Only PSB 603, the A_{2B}AR selective antagonist, inhibited the NECA response, confirming the A_{2B}AR specific hypothesis (Figure 5). As a result, further experiments for the study of A_{2B}AR were performed on CHO-spap-hA_{2B}AR cells.

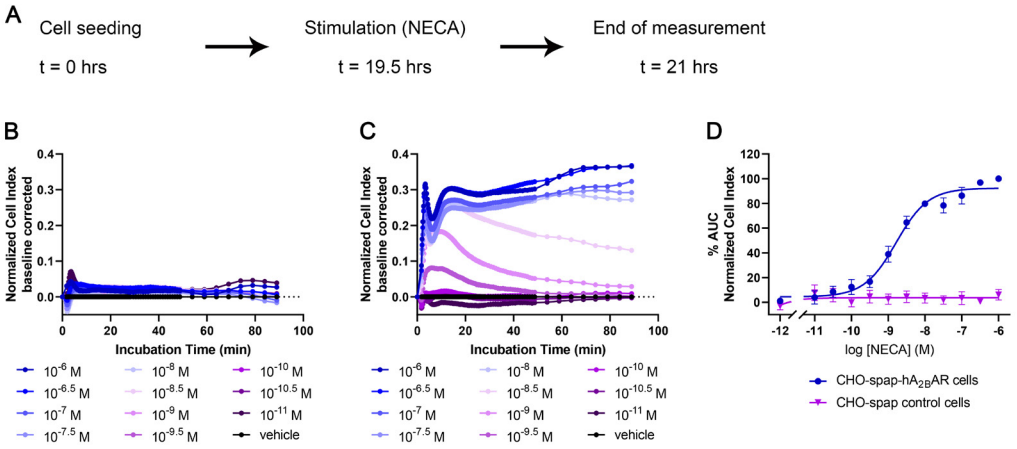

Figure 4: Functional characterization of NECA on CHO-spap and CHO-spap-hA_{2B}AR cells. (A) Graphic representation of assay set-up. Cell were seeded and 19.5 hours later they were stimulated with NECA (10 pM – 1 µM) and the cell response was monitored for 1.5 hours. Representative responses induced by NECA on (B) CHO-spap and (C) CHO-spap-hA_{2B}AR cells. (D) Concentration-response curves of NECA. The curves were normalized to minimum (0%) to maximum response (100%) of CHO-spap-hA_{2B}AR cells. Data shown are mean ± SEM from at least three separate experiments performed in duplicate.

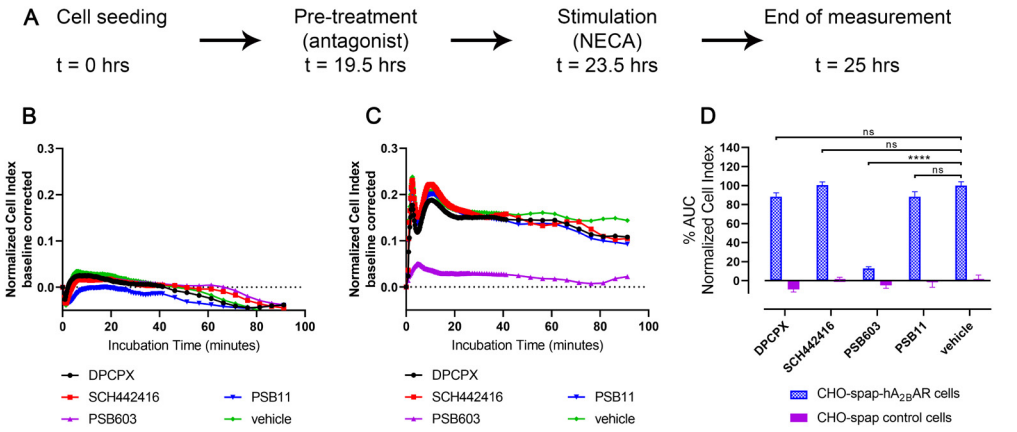

Figure 5: NECA activation signaling on CHO-spap and CHO-spap-hA_{2B}AR cells is only mediated via hA_{2B}AR. (A) Graphic representation of assay set-up. Cell were seeded and 19.5 hours later they were pre-treated with an antagonist for all ARs (A_1: DPCPX; A_{2A}: SCH 442416; A_{2B}: PSB 603; A3: PSB 11). Later they were stimulated with an EC_{80} concentration of NECA (4 nM) and the cell response was monitored for 1.5 hours. Representative responses induced by NECA on (B) CHO-spap and (C) CHO-spap-hA_{2B}AR cells. (D) Bar graphs represent the AUC of antagonists for all ARs after stimulation with EC_{80} of NECA. The data were normalized to vehicle 1 treated with NECA of CHO-spap-hA_{2B}AR cells as 100%. Data shown are mean ± SEM from at least three separate experiments performed in duplicate. ns P >0.05, *** $P \leq$ 0.001 determined in a one-way ANOVA test with Dunnett's correction.

After this assay development, compounds **17** and **18**, with an 11-fold difference in RT, were selected for further experiments. First, their inhibitory potency in the presence of an EC_{80} concentration of NECA was determined resulting in pIC_{50} values of 7.12 ± 0.13 and 6.44 ± 0.21, respectively (Figure 6, Table 5). These potencies were found to be approximately 1.5 log unit lower than their affinities determined in the radioligand binding studies (8.64 ± 0.05 and 7.70 ± 0.06 for **17** and **18**, respectively; Table 3), in line with the presence of a high agonist concentration (*i.e.* EC_{80}) in this assay set-up.

Subsequently, a washout assay was performed and the cell response to the compounds was monitored and evaluated (Figure 7). In short, cells were pre-treated with a concentration of 30 x IC_{50} of the compounds and 4 hr later cells were washed and fresh "no serum" medium was added. For the evaluation of the unwashed condition, the medium was not refreshed but was pipetted up and down in order to mimic the possible mechanical stress induced to the washed cells. Cells were then stimulated with an EC_{80} concentration of NECA, enabling us to monitor the response exerted by only those receptors that were not bound to compounds **17** and **18**. Based on the experimental set-up, it was hypothesized that the short RT compound was removed more readily during washing, resulting in an increased number of receptors available for NECA to bind and cause a cellular response.

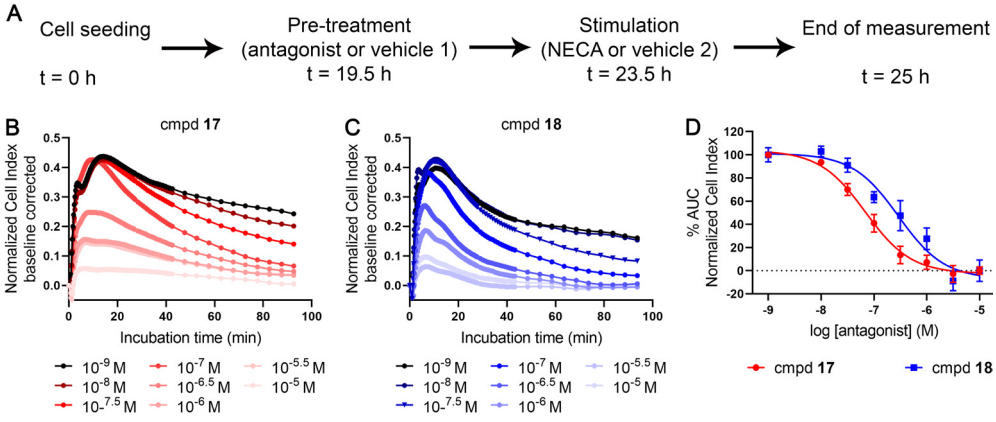

Figure 6: Functional characterization of compound **17** (short RT) and **18** (long RT) on CHO-spap-hA_{2B}AR cells. (A) Graphic representation of assay set-up. Cell were seeded and 19.5 hr later they were pre-treated with antagonist **17** or **18** (1 nM - 10 µM) or control (vehicle 1; 0.25% DMSO). After a 4 hr incubation, cells were stimulated with an EC_{80} concentration of NECA (4 nM) or control (vehicle 2; 0.25% DMSO) and the cell response was monitored for 1.5 hr. (B, C) Representative responses induced by NECA after pre-treatment with various concentrations of compound **17** (B) and compound **18** (C). (D) Concentration-response curves of antagonists after stimulation with EC_{80} concentration of NECA. The curves were normalized to minimum (0%) and maximum response (100%). Data shown are mean ± SEM from at least three separate experiments performed in duplicate.

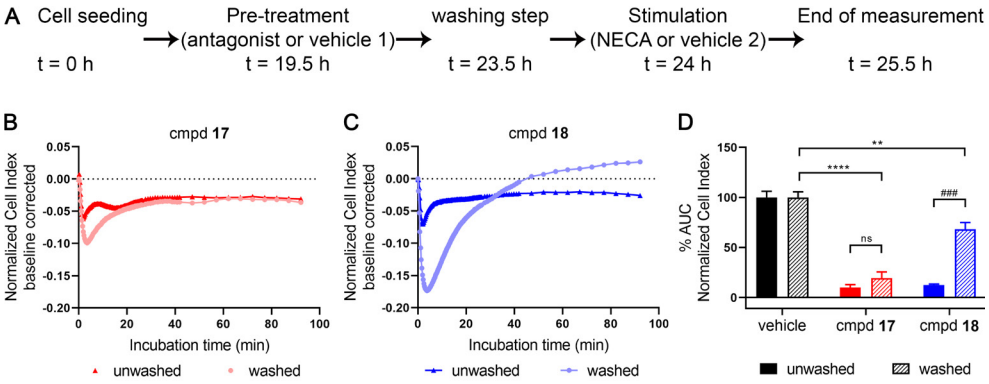

Figure 7: Recovery of NECA signaling after washing. (A) Graphic representation of assay set-up. Cell were seeded and 19.5 hr later they were pre-treated with an antagonist (30 x IC_{50} as determined in the label-free assay in Figure 6) or control (vehicle 1; 0.25% DMSO). After a 4 hr incubation, cells were washed by removing the medium from the well and replacing it with 95 µL of fresh serum-free medium. For the unwashed condition, no medium refreshment was done. 30 min afterwards, cells were treated with NECA (at an EC_{80} concentration) or control (vehicle 2; 0.25% DMSO) and the cell response was monitored for 1.5 hr. (B,C) Representative responses induced by NECA with or without washing of cells pre-treated with compound **17** (B) and compound **18** (C). (D) Bar graph showing NECA response after washing step when cells were pre-treated with compound **17** or **18**. Bar graphs of both washed and unwashed conditions were compared to the control (vehicle) without any antagonist (100% washed and unwashed AUC, respectively). Data shown are mean ± SEM from at least three separate experiments performed in duplicate. ns $P > 0.05$, $^{###}$ $P \leq 0.001$ determined in an unpaired t-test with Welch's correction. ** $P \leq 0.01$, **** $P \leq 0.0001$ determined in a one-way ANOVA test with Dunnett's correction.

Table 5: Radioligand binding data at $hA_{2B}AR$ cell membranes before and after washing, potency values (pEC_{50} and pIC_{50}) of compounds in a label-free assay, and NECA signaling therein before and after washing, all on CHO-spap-$hA_{2B}AR$ cells.

cmpd	Radioligand binding assay		Label-free assay			
	washout - % binding		pEC_{50} (EC_{50} (nM))	pIC_{50} (IC_{50} (nM))	washout - %AUC	
	unwashed	3x washed			unwashed	1x washed
NECA	n.a.	n.a.	8.95 ± 0.13 (1.12)	n.a.	100	100
17	-2 ± 1	42 ± 2	n.a	7.12 ± 0.13 (75.4)	10 ± 3	19 ± 6
18	-8 ± 1	103 ± 3	n.a.	6.44 ± 0.21 (363)	12 ± 1	68 ± 7

Values represent the mean ± SEM of at least three individual experiments, performed in duplicate. n.a. = not applicable.

Cells pre-treated with long RT compound **17** showed no significant increase ($p>0.05$) in NECA signaling after washing (9.8% and 12% for unwashed and washed cells, respectively) (Figure 7C, Table 5). On the contrary, the increase in NECA signaling between unwashed and washed cells was significantly higher ($P < 0.001$) with the short RT compound **18** (19% and 68% for unwashed and washed cells, respectively) (Figure 7C, Table 5), verifying our hypothesis. This assay simulates a non-equilibrium condition, not unlike human physiology. As a result, findings from this assay constitute a possible translational step towards *in vivo* experiments[48].

Conclusions

In this study, we reported the synthesis and pharmacological evaluation of a series of xanthine-based analogues designed as $hA_{2B}AR$ antagonists. A radioligand competition association assay was developed to evaluate kinetic binding parameters next to affinity. Structure-affinity and structure-kinetic relationships (SAR and SKR) were examined and a great spread in target residence time (RT) was observed, from 0.9 min (**3**) to 87 min (**17**). Based on correlation plots, the dissociation rate constant appeared the driving force for affinity unlike the association rate constants. Subsequently two compounds (**17** and **18**) with long and short RT, respectively, were selected and tested in a label-free impedance-based assay. These experiments confirmed the link between long RT and an extended pharmacological effect under non-equilibrium conditions. To our knowledge, this is the first SKR study performed on $hA_{2B}AR$ antagonists, which could pave the way to the development of antagonists with a high affinity and long residence time at the $A_{2B}AR$.

Experimental Section

CHEMISTRY.

Compounds **2**, **8**, **11** - **19**, **26** and **27** were reported in Kim *et al.*[21].

General procedure for the preparation of benzylamide derivatives 3-7, 9, 10, 20-25.

A solution of XCC (1, 8-[4-[carboxymethyloxy]phenyl]-1,3-di-(n-propyl)xanthine (1 eq)[49], the desired amine compound (1 eq), EDAC (1-ethyl-3-(2-dimethylaminoethyl) carbodiimide, 2 eq.) and DMAP (4-[N,N-(dimethylamino)]pyridine, 2.2 eq) in 2 mL of anhydrous dimethylformamide was stirred at room temperature for 24 hr. The reaction mixture was evaporated to dryness under a stream of nitrogen, and the residue was

purified by preparative silica gel thin layer chromatography (chloroform:methanol = 20:1) and crystallization in methanol/ethyl ether to afford the desired compounds.

N-cyclopropyl-2-(4-(2,6-dioxo-1,3-dipropyl-2,3,6,7-tetrahydro-1H-purin-8-yl) phenoxy)acetamide (3, MRS 1862). Compound **3** was synthesized following the general procedure using cyclopropilamine and obtaining 15.0 mg of pure compound (68% yield). ^{1}H NMR (DMSO, 400 Hz) δ 8.17 (d, 1H, J = 3.3 Hz), 8.06 (d, 2H, J = 8.7 Hz), 7.06 (d, 2H, J = 8.7 Hz, 2H), 4.51 (s, 2H), 4.01 (t, 2H, J = 7.1 Hz), 3.86 (t, 2H, J = 7.3 Hz), 3.87 (t, 2H, J = 7.3 Hz), 2.67-2.71 (m, 1H), 1.73 (q, 2H, J = 7.4, 14.5 Hz), 1.57 (q, 2H, J = 7.4, 14.5 Hz), 0.85-0.92 (m, 6H), 0.61-0.66 (m, 2H), 0.46-0.50 (m, 2H). HRMS calcd $C_{22}H_{28}N_5O_4$ $(M+H)^+$: 426.2141, found 426.2139

N-cyclobutyl-2-(4-(2,6-dioxo-1,3-dipropyl-2,3,6,7-tetrahydro-1H-purin-8-yl) phenoxy)acetamide (4, MRS 1867). Compound **4** was synthesized following the general procedure using cyclobutylamine and obtaining 19.0 mg of pure compound (95% yield). ^{1}H NMR (DMSO + $CDCl_3$, 300 Hz) δ 8.26 (d, 1H, J = 8.1 Hz), 8.60 (d, 2H, J = 9.0 Hz), 7.59 (d, 2H, J = 9.0 Hz), 4.49 (s, 2H), 4.28 (dd, 1H, J = 7.5, 16.2 Hz), 4.20 (t, 2H, J = 7.2 Hz), 3.88 (t, 2H, J = 7.4 Hz), 2.1-2.2 (m, 2H), 1.94-2.4 (m, 2H), 1.71-1.80 (m, 2H), 1.54-1.71 (m, 4H), 0.92 (t, 3H, J = 5.1 Hz), 0.87 (t, 3H, J = 5.1 Hz). HRMS calcd $C_{24}H_{23}N_6O_4$ $(M+H)^+$: 459.1781; found 459.1779.

N-cyclopentyl-2-(4-(2,6-dioxo-1,3-dipropyl-2,3,6,7-tetrahydro-1H-purin-8-yl) phenoxy)acetamide (5, MRS 1863). Compound **5** was synthesized following the general procedure using cyclopentylamine and obtaining 20.0 mg of pure compound (85% yield). ^{1}H NMR (DMSO, 400 Hz) δ 8.06 (d, 2H, J = 8.7 Hz), 8.01 (d, 1H, J = 5.3 Hz), 7.06 (d, 2H, J = 8.8 Hz, 2H), 4.52 (s, 2H), 3.99-4.08 (m, 4H), 3.84 (t, 4H, J = 7.4 Hz), 1.40-1.82 (m, 12H), 0.85-0.92 (m, 6H). HRMS calcd $C_{24}H_{32}N_5O_4$ $(M+H)^+$: 454.2454; found 454.2457.

2-(4-(2,6-dioxo-1,3-dipropyl-2,3,6,7-tetrahydro-1H-purin-8-yl)phenoxy)-N-(1H-pyrazol-3-yl)acetamide (6, MRS 1827). Compound **6** was synthesized following the general procedure using 3-aminopyrazole and obtaining 5.0 mg of pure compound (21% yield). ^{1}H NMR (DMSO, 400 Hz) δ 12.39 (s, 1H), 10.56 (s, 1H), 8.07 (d, 2H, J = 8.7 Hz), 7.62 (s, 1H), 7.09 (d, 2H, J = 8.6 Hz, 2H), 6.49 (s, 1H), 4.77 (s, 2H), 4.01 (s, 2H), 3.86 (t, 2H, J = 7.2 Hz), 1.72 (q, 2H, J = 7.4, 14.5 Hz), 1.57 (q, 2H, J = 7.3, 14.4 Hz), 0.85-0.92 (m, 6H). HRMS calcd $C_{22}H_{26}N_7O_4$ $(M+H)^+$: 452.2046; found 452.2047.

N-cyclohexyl-2-(4-(2,6-dioxo-1,3-dipropyl-2,3,6,7-tetrahydro-1H-purin-8-yl) phenoxy)acetamide (7, MRS 1864). Compound **7** was synthesized following the general procedure using cyclohexylamine and obtaining 19.0 mg of pure compound (79% yield). ^{1}H NMR (DMSO, 400 Hz) δ 8.06 (d, 2H, J = 8.7 Hz), 7.92 (d, 1H, J = 8.2 Hz), 7.07 (d, 2H, J = 8.7 Hz, 2H), 4.52 (s, 2H), 4.01 (t, 2H, J = 7.2 Hz), 3.86 (t, 2H, J = 7.3 Hz), 3.61 (s, 1H), 1.66-1.76 (m, 5H), 1.55-1.63 (m, 3H), 1.24-1.26 (m, 3H), 1.10-1.12 (m, 1H), 0.85-0.92 (m, 6H). HRMS calcd $C_{25}H_{34}N_5O_4$ $(M+H)^+$: 468.2611; found 468.2618.

2-(4-(2,6-dioxo-1,3-dipropyl-2,3,6,7-tetrahydro-1H-purin-8-yl)phenoxy)-N-(pyridin-4-ylmethyl)acetamide (9, MRS 1826). Compound **9** was synthesized following the general procedure using 4-(methylamino)pyridine and obtaining 11.0 mg of pure compound (45% yield). ^{1}H NMR (DMSO, 400 Hz) δ 8.79 (t, 1H, J = 5.7 Hz), 8.47 (d, 2H, J = 5.6 Hz), 8.08 (d, 2H, J = 8.8 Hz), 7.23 (d, 1H, J = 5.5 Hz), 7.12 (d, 2H, J = 8.7 Hz, 2H), 4.68 (s, 2H), 4.37 (d, 2H, J = 6.1 Hz), 4.02 (t, 2H, J = 7.2 Hz), 3.87 (t, 2H, J = 7.0 Hz), 1.74 (q, 2H, J = 7.4, 14.5 Hz), 1.58 (q, 2H, J = 7.3, 14.4 Hz), 0.85-0.92 (m, 6H). HRMS calcd $C_{25}H_{29}N_6O_4$ $(M+H)^+$: 477.2250; found 477.2243.

2-(4-(2,6-dioxo-1,3-dipropyl-2,3,6,7-tetrahydro-1H-purin-8-yl)phenoxy)-N-(pyrazin-2-yl)acetamide (10, MRS 1825). Compound **10** was synthesized following the general procedure using aminopyrazine and obtaining 6.5 mg of pure compound (27% yield). ^{1}H NMR (DMSO, 400 Hz) δ 10.97 (s, 1H), 9.30 (s, 1H), 8.44 (s, 1H), 8.40 (s, 1H), 8.07 (d, 2H, J = 8.7 Hz), 7.11 (d, 2H, J = 8.7 Hz, 2H), 4.94 (s, 2H), 2.38 (t, 2H, J = 7.1 Hz), 3.86 (t, 2H, J = 7.2 Hz), 1.73 (q, 2H, J = 7.4, 14.5 Hz), 1.58 (q, 2H, J = 7.3, 14.4 Hz), 0.85-0.92 (m, 6H). HRMS calcd $C_{23}H_{26}N_7O_4$ $(M+H)^+$: 464.2046; found 464.2047.

2-(4-(2,6-dioxo-1,3-dipropyl-2,3,6,7-tetrahydro-1H-purin-8-yl)phenoxy)-N-(4-methylbenzyl)acetamide (20, MRS 1886). Compound **20** was synthesized following the general procedure using 4-methylbenzylamine and obtaining 44.5 mg of pure compound (91% yield). ^{1}H NMR (DMSO, 300 Hz) δ 8.64 (t, 1H, J = 5.9 Hz), 8.07 (d, 2H, J = 8.8 Hz), 7.16 – 7.08 (m, 6H), 4.63 (s, 2H), 4.30 (d, 2H, J = 5.9 Hz), 4.02 (t, 2H, J = 7.0 Hz), 3.87 (t, 2H, J = 7.3 Hz), 2.26 (s, 3H), 1.74 (m, 2H), 1.58 (m, 2H), 0.91 (t, 3H, J = 7.6 Hz), 0.88 (t, 3H, J = 7.7 Hz). HRMS calcd $C_{27}H_{32}N_5O_4$ $(M+H)^+$: 490.2454; found 490.2462.

2-(4-(2,6-dioxo-1,3-dipropyl-2,3,6,7-tetrahydro-1H-purin-8-yl)phenoxy)-N-(4-fluorobenzyl)acetamide (21, MRS 1891). Compound **21** was synthesized following the general procedure using 4-fluorobenzylamine and obtaining 32.3 mg of pure compound (65% yield). ^{1}H NMR (DMSO, 300 Hz) δ 8.71 (t, 1H, J = 5.9 Hz), 8.07 (d, 2H, J = 8.8 Hz), 7.30 (dd, 2H, J = 5.9, 8.5 Hz), 7.16-7.08 (m, 4H), 4.64 (s, 2H), 4.33 (d, 2H, J = 6.0 Hz), 4.02 (t, 2H, J = 7.1 Hz), 3.87 (t, 2H, J = 7.3 Hz), 1.74 (m, 2H), 1.58 (m, 2H), 0.91 (t, 3H, J = 7.6 Hz), 0.88 (t, 3H, J = 7.6 Hz). HRMS calcd $C_{26}H_{29}FN_5O_4$ $(M+H)^+$: 494.2204; found 494.2199.

N-(4-bromobenzyl)-2-(4-(2,6-dioxo-1,3-dipropyl-2,3,6,7-tetrahydro-1H-purin-8-yl)phenoxy)acetamide (22, MRS 1878). Compound **22** was synthesized following the general procedure using 4-bromobenzylamine and obtaining 30.0 mg of pure compound (54% yield). ^{1}H NMR (DMSO, 300 Hz) δ 8.75 (t, 1H, J = 6.1 Hz), 8.09 (d, 2H, J = 8.7 Hz), 7.47-7.40 (m, 2H), 7.27 (d, 2H, J = 4.9 Hz), 7.10 (d, 2H, J = 8.9 Hz), 4.66 (s, 2H), 4.35 (d, 2H, J = 6.1 Hz), 4.02 (t, 2H, J = 7.1 Hz), 3.87 (t, 2H, J = 7.3 Hz), 1.74 (m, 2H), 1.58 (m, 2H), 0.91 (t, 3H, J = 7.5 Hz), 0.88 (t, 3H, J = 7.6 Hz). HRMS calcd $C_{26}H_{29}BrN_5O_4$ $(M+H)^+$: 554.1403; found 554.1397.

N-(3,4-dihydroxybenzyl)-2-(4-(2,6-dioxo-1,3-dipropyl-2,3,6,7-tetrahydro-1H-

purin-8-yl)phenoxy)acetamide (23, MRS 1883). Compound **23** was synthesized following the general procedure using 3,4-dihydroxybenzylamine hydrobromide and obtaining 18.7 mg of pure compound (37% yield). ^{1}H NMR (DMSO, 300 Hz) δ 8.53 (t, 1H, J = 6.0 Hz), 8.06 (d, 2H, J = 8.9 Hz), 7.08 (d, 2H, J = 8.8 Hz), 6.69 (d, 1H, J = 1.8 Hz), 6.65 (d, 1H, J = 8.0 Hz), 6.51 (dd, 1H, J = 8.1, 1.9 Hz), 4.59 (s, 2H), 4.17 (d, 2H, J = 6.0 Hz), 4.01 (t, 2H, J = 7.2 Hz), 3.86 (t, 2H, J = 7.3 Hz), 1.74 (m, 2H), 1.58 (m, 2H), 0.90 (t, 3H, J = 7.4 Hz), 0.87 (t, 3H, J = 7.6 Hz). HRMS calcd $C_{26}H_{30}N_5O_6$ $(M+H)^+$: 508.2196; found 508.2184.

(R)-2-(4-(2,6-dioxo-1,3-dipropyl-2,3,6,7-tetrahydro-1H-purin-8-yl)phenoxy)-N-(1-phenylethyl)acetamide (24, MRS 1892). Compound **24** was synthesized following the general procedure using R-(+)-α-methylbenzylamine and obtaining 28.6 mg of pure compound (58% yield). ^{1}H NMR (DMSO, 300 Hz) δ 8.57 (d, 1H, *J* = 8.4 Hz), 8.06 (d, 2H, *J* = 8.7 Hz), 7.33-7.20 (m, 5H), 7.08 (d, 2H, *J* = 8.7 Hz), 5.01 (m, 1H), 4.61 (s, 2H), 4.02 (t, 2H, *J* = 7.1 Hz), 3.87 (t, 2H, *J* = 7.3 Hz), 1.74 (m, 2H), 1.58 (m, 2H), 1,41 (d, 3H, *J* = 6.9 Hz), 0.90 (t, 3H, *J* = 7.6 Hz), 0.88 (t, 3H, *J* = 7.8 Hz). HRMS calcd $C_{27}H_{32}N_5O_4$ $(M+H)^+$: 490.2454; found 490.2433.

(S)-2-(4-(2,6-dioxo-1,3-dipropyl-2,3,6,7-tetrahydro-1H-purin-8-yl)phenoxy)-N-(1-phenylethyl)acetamide (25, MRS 1893). Compound **25** was synthesized following the general procedure using S-(-)-α-methylbenzylamine and obtaining 22.0 mg of pure compound (45% yield). ^{1}H NMR (DMSO, 300 Hz) δ 8.57 (d, 1H, *J* = 8.1 Hz), 8.06 (d, 2H, *J* = 8.7 Hz), 7.33-7.20 (m, 5H), 7.08 (d, 2H, *J* = 8.7 Hz), 5.01 (m, 1H), 4.61 (s, 2H), 4.02 (t, 2H, *J* = 7.1 Hz), 3.87 (t, 2H, *J* = 7.2 Hz), 1.74 (m, 2H), 1.58 (m, 2H), 1,41 (d, 3H, *J* = 7.0 Hz), 0.90 (t, 3H, *J* = 7.6 Hz), 0.88 (t, 3H, *J* = 7.7 Hz). HRMS calcd $C_{27}H_{32}N_5O_4$ $(M+H)^+$: 490.2454; found 490.2429.

BIOLOGY.

Chemicals and Reagents.

Bovine serum albumin (BSA) and the bicinchoninic acid (BCA) protein assay kit were purchased from Fisher Scientific (Hampton, New Hampshire, United States). [^{3}H]PSB-603 precursor was kindly synthesized by the group of Prof. Christa Müller (University of Bonn), custom-labeled (specific activity 79 Ci mmol^{-1}) and purchased from Quotient Bioresearch (Cardiff, UK), while ZM241385 was a kind gift by Zeneca Pharmaceuticals (Macclesfield, UK). Adenosine deaminase (ADA) was purchased from Sigma Aldrich (Zwijndrecht, the Netherlands). CHO-spap cells stably expressing the wildtype human A_{2B}AR (CHO-spap-hA_{2B}AR) were kindly provided by S.J. Dowell, Glaxo Smith Kline. All other chemicals were purchased from standard commercial sources.

Cell culture.

CHO-spap cells were grown in Dulbecco's modified Eagle's medium: Nutrient Mixture F-12 (DMEM/F12) supplemented with 10% (v/v) newborn calf serum, 100 IU/mL penicillin and 100 µg/mL streptomycin at 37 °C and 5% CO_2. Cells were subcultured at a ratio of 1:20 twice weekly.

CHO-spap-hA_{2B}AR cells were grown in the same medium supplemented with 1 mg/mL G418 and 0.4 mg/mL hygromycin. Cells were subcultured at a ratio of 1:20 twice weekly.

Membrane Preparation.

CHO-spap-hA_{2B}AR cells were cultured as a monolayer in 15 cm ø plates to about 90% confluency. Cells were removed from the plates by scraping into 5 mL of phosphate-buffered saline (PBS) and centrifuged for 5 min at 1500 rpm. The resulting pellets were resuspended in ice-cold Tris-HCl buffer (50 mM Tris-HCl, pH 7.4) and homogenized using an Ultra Turrax homogenizer (IKA Werke GmbH & Co.KG, Staufen, Germany). Centrifugation at 31,000 rpm in an Optima LE-80 K ultracentrifuge with Ti-70 rotor (Beckman Coulter, Fullerton, CA) at 4°C for 20 min, resulted in separation of membranes and cytosolic fraction. Subsequently, pellet was resuspended in 10 mL Tris-HCl buffer, homogenized and centrifuged once again. The final pellet was suspended in assay buffer (50 mM Tris-HCl buffer, 0.1% (w/v) CHAPS, pH 7.4), ADA was added to break down endogenous adenosine, and the homogenization step was repeated. Aliquots were stored at -80°C and the membrane protein concentration was determined by a BCA protein determination assay[50]. The BCA results were measured in a Wallac EnVision 2104 Multilabel Reader (Perkin Elmer, Groningen, The Netherlands).

Radioligand Binding assay.

In all radioligand binding experiments, CHO-spap-hA_{2B}AR membranes were thawed and homogenized using an Ultra Turrax homogenizer at 24,000 rpm (IKA-Werke GmbH & Co.KG, Staufen, Germany), diluted in assay buffer to the desired concentration (10-30 µg per well or Eppendorf tube). All materials were brought to 25 °C, 30 min prior to the experiment. ZM 241385 (10 µM) was used to determine nonspecific binding (NSB). DMSO concentrations were 2% for all compounds except for 8, 12-18 and 20-22, where the concentration was 0.25%. The two different DMSO concentrations had negligible effects on the radioligand binding results. Finally, total radioligand binding (TB) did not exceed 10% of the [^{3}H]PSB 603 present in the assay in order to prevent ligand depletion.

Displacement experiments were performed using 1.5 nM [^{3}H]PSB 603 and a competing unlabeled ligand at multiple concentrations diluted in assay buffer. Binding

was initiated by addition of CHO-spap-hA_{2B}AR membrane aliquots to reach a total volume of 100 µL. Samples were incubated at 25 °C for 2 h to reach equilibrium. The incubation was terminated by rapid vacuum filtration over 96-well Whatman GF/C filter plates using a PerkinElmer Filtermate harvester (PerkinElmer, Groningen, Netherlands). Filters were subsequently washed ten times using ice-cold wash buffer (50 mM Tris-HCl, 0.1% (w/v) BSA, pH 7.4). Filter plates were dried at 55 °C for about 45 min and afterwards 25 µL Microscint (PerkinElmer) was added per well. Filter-bound radioactivity was determined by liquid scintillation spectrometry using a 2450 Microbeta^2 scintillation counter (PerkinElmer).

Saturation binding experiments were carried out by incubating increasing concentrations of [^{3}H]PSB 603 (from 0.05 to 5 nM) with membrane aliquots for 2 hr at 25 °C. Non-specific binding was assessed by three concentrations of the radioligand (0.05 nM, 1 nM and 5 nM) and analyzed by linear regression. Incubation was terminated by filtration through GF/C filters using a Brandel-harvester (Brandel Harvester 24w, Gaithersburg, MD, USA). Filters were washed three times using ice-cold washing buffer and collected in tubes. 3.5 mL Emulsifier-Safe scintillation fluid (Perkin Elmer, Groningen, the Netherlands) was added and the filter-bound radioactivity was determined in a Tri-Carb 2900TR liquid scintillation analyzer (PerkinElmer).

Association experiments were performed by incubation of [^{3}H]PSB 603 (1.5 nM) with membrane aliquots at 25 °C. The amount of receptor-bound radioligand was determined after filtration at different time intervals for a total incubation time of 45 min and samples were obtained as described under “Displacement experiments”.

Dissociation experiments were carried out after a 45 min pre-incubation of 1.5 nM [^{3}H]PSB 603 and membrane aliquots. Subsequently, dissociation of the radioligand at different time points up to 150 min was initiated by addition of 5µL ZM 241385 (assay concentration 10 µM). Dissociation experiments were performed at 25 °C. The amount of receptor-bound radioligand was determined after filtration and samples were obtained as described under “Displacement experiments”.

Competition association experiments were performed at 25 °C and in a total volume of 100 µL, by incubation of 1.5 nM [^{3}H]PSB 603 and a competing ligand diluted in assay buffer to reach IC_{50} concentration. Addition of CHO-spap-hA_{2B}AR membrane aliquots initiated the binding. The amount of receptor-bound radioligand was determined at different time points up to 3 hr. After 3 hr the incubation was terminated and samples were obtained as described under “*displacement experiments”*.

Washout experiments were performed at 25 °C and in a total volume of 400 µL. CHO-spap-hA_{2B}AR membranes were incubated for 2 hr with the unlabeled compounds (at a final concentration of 10 × IC_{50}) while shaking at 1,000 RPM in an Eppendorf thermomixer comfort (Eppendorf AG, Hamburg, Germany). Subsequently, the samples were centrifuged at 13200 rpm (16 100g) at 4 °C for 5 min and the supernatant containing unbound ligand was removed. Pellets were resuspended

in 1 mL of assay buffer, and samples were incubated for 10 min at 25 °C in the thermomixer. After three centrifugation and washing cycles in total, supernatant was discarded and the membranes were resuspended in a total volume of 400 µL containing 1.5 nM [^{3}H]PSB 603. After 2 hr at 25 °C incubations were terminated by rapid filtration through GF/C filters using a Brandel harvester and the samples were obtained as described under “saturation experiments”.

Label-free whole-cell assay.

Detection principle. Label-free assays were performed using the xCELLigence real-time cell analyser (RTCA) system[39, 40], as described previously[51]. In short, cells attached to the gold-coated electrodes embedded on the bottom of E-plates are generating electrical impedance which is monitored by the RTCA system. Variations in cell number, adhesion, viability and morphology result in impedance changes (Z) which are constantly recorded at 10 kHz. Z is displayed in the unitless parameter called Cell Index (CI)[40, 41], which is defined as $(Z_i\text{-}Z_0)$ Ω /15 Ω. Z_i is the impedance at a given time point and Z_0 represents the baseline impedance in the absence of cells, which is measured prior to the start of the experiment.

Determination of pEC_{50} value of NECA for $hA_{2B}AR$. CHO-spap and CHO-spap-hA_{2B}AR cells were harvested and centrifuged at 200x *g* (1500 rpm) for 5 min. Z_0 was measured in the presence of 45 µL culture media in 96 well PET E-plates (Bioké, Leiden). 60,000 cells were seeded in a volume of 50 µL per well. After maintaining at room temperature for about 30 min, the E-plate was placed into the recording station housed in a 37°C and 5% CO_2 incubator. Impedance was measured every 15 min. After about 19 hr 30 min of recording, cells were treated with NECA (10^{-11} till 10^{-6} M) or vehicle control (0.25% DMSO) in 5 µL. CI was recorded for 90 min (recording schedule: 15 second intervals for 25 min, followed by 1 min intervals for 20 min and 5 min intervals for 45 min).

Validation that NECA signaling is $hA_{2B}AR$-mediated. Z_0 was measured in the presence of 45 µL culture media in 96 well PET E-plates (Bioké, Leiden). 60,000 CHO-spap or CHO-spap-hA_{2B}AR cells were seeded in a volume of 50 µL per well. The E-plate was left for about 30 min at room, and afterwards was placed into the recording station housed in a 37°C and 5% CO_2 incubator. Impedance measurements were recorded every 15 min. After about 19 hr 30 min of recording, cells were pre-treated with saturating concentrations of an AR antagonist, *i.e.* A_1: DPCPX (45 nM); A_{2A}: SCH 442416 (4.8 nM); A_{2B}: PSB 603 (55 nM); A3: PSB 11 (230 nM) or vehicle control (vehicle 1; 0.25% DMSO) in 5 µL. CI was recorded for 4 hr (recording schedule: 15 second intervals for 10 min, followed by 1 min intervals for 50 min and 15 min interval for 180 min). Subsequently, cells were treated with NECA (EC_{80}) or vehicle control (vehicle 2; 0.25% DMSO) in 5 µL and CI was recorded for 90 min (recording schedule: 15 second intervals for 25 min, followed by 1 min intervals for 15 min and 5 min intervals for 50 min).

Determination of pIC_{50} values of $hA_{2B}AR$ antagonists. Z_0 was measured in the presence of 40 µL culture media in 96 well PET E-plates (Bioké, Leiden). CHO-spap-$hA_{2B}AR$ cells were seeded in a density of 60,000 cells per well (50 µL). After staying 30 min without agitation at room temperature, the E-plate was placed into the recording station housed in a 37°C and 5% CO_2 incubator. Impedance was measured every 15 min. After about 19 hr 30 min of recording, cells were pre-treated with $A_{2B}AR$ antagonists (10^{-9} till 10^{-5} M) or vehicle control (vehicle 1; 0.25% DMSO) in 5 µL. CI was recorded for 4 hr (recording schedule: 15 second intervals for 10 min, followed by 1 min intervals for 50 min and 15 min interval for 180 min). Subsequently, cells were treated with NECA (EC_{80}) or vehicle control (vehicle 2; 0.25% DMSO) in 5 µL and CI was recorded for 90 min (recording schedule: 15 second intervals for 25 min, followed by 1 min intervals for 15 min and 5 min intervals for 50 min).

Washout assay. The assay followed the same initial steps as described in "*Determination of pIC_{50} values for $hA_{2B}AR$ antagonists"*. After about 19 hr 30 min of recording, cells were pre-treated with $A_{2B}AR$ antagonists (30 x IC_{50}; based on the pIC_{50} value determined with "*Determination of pIC_{50} values for $hA_{2B}AR$ antagonists"*) or vehicle control (vehicle 1; 0.25% DMSO) in 5 µL. CI was recorded for 4 hr (recording schedule: 15 second intervals for 10 min, followed by 1 min intervals for 50 min and 15 min intervals for 180 min). Subsequently, wells were washed by aspiration of the medium, followed by the addition of 95 µL fresh serum free medium. For the unwashed cells, the medium was not removed but was pipetted up and down to simulate any mechanical cell stress. The E-plate was placed on the recording station and CI was recorded for 30 min (recording schedule: 15 second intervals for 25 min, followed by 1 min intervals for 5 min). Finally, cells were treated with NECA (EC_{80}) or vehicle control (vehicle 2; 0.25% DMSO) in 5 µL and CI was recorded for 90 min (recording schedule: 15 second intervals for 25 min, followed by 1 min intervals for 15 min and 5 min intervals for 50 min).

Data analysis

Radioligand binding assays.

Data analyses were performed using GraphPad Prism 8.0 software (GraphPad Software Inc., San Diego, CA, USA). For saturation assays, K_D and B_{max} values were determined by non-linear regression curve fitting using the one site: "total and non-specific binding" equation. For displacement assays, pIC_{50} values were obtained by non-linear regression curve fitting to a sigmoidal concentration-response curve using the "log(inhibitor) vs. response" GraphPad analysis equation. pK_i values were converted from pIC_{50} values and the saturation K_D using the ChengPrusoff equation[52]: $K_i = IC_{50} / (1 + [\text{radioligand}] / K_D)$.

The k_{off} value was obtained using a one-phase exponential decay analysis of data resulting from a radioligand dissociation assay. The value of k_{on} was determined

using the equation:

$k_{on} = (k_{obs} - k_{off}) / [\text{radioligand}]$,

in which k_{obs} was determined using a one phase association analysis of data from a radioligand association assay. The association and dissociation rate constants were used to calculate the kinetic K_D value using: $K_D = k_{off} / k_{on}$.

Association and dissociation rate constants for unlabelled A_{2B}AR inhibitors were determined by nonlinear regression analysis of competition association data as described by Motulsky and Mahan[23]. The data were fitted into the GraphPad "kinetics of competitive binding" analysis, where k_1 and k_2 are the k_{on} ($M^{-1}min^{-1}$) and k_{off} (min^{-1}) of [^{3}H]PSB 603 obtained from radioligand association and dissociation assays, respectively, L is the radioligand concentration (nM), I is the concentration of unlabeled competitor (nM), X is the time (min) and Y is the specific binding of the radioligand (DPM). Fixing these parameters resulted in the calculation of the following parameters: k_3, which is the k_{on} value ($M^{-1}min^{-1}$) of the unlabeled ligand; k_4, which is the k_{off} value (min^{-1}) of the unlabeled ligand and B_{max}, that equals the total binding (DPM). All competition association data were globally fitted. The residence time (RT) was calculated using $RT = 1 / k_{off}$ [53].

All values are shown as mean ± S.E.M. of at least three independent experiments performed in duplicate. Statistical analysis was performed if indicated, using a one-way ANOVA with Dunnett's post-test (**** $P < 0.0001$; *** $P < 0.001$; ** $P < 0.01$; * $P < 0.05$) or an unpaired Student's t test (#### $P < 0.0001$; ### $P < 0.001$; ## $P < 0.01$; # $P < 0.05$). Observed differences were considered statistically significant if P-values were below 0.05.

Label-free whole-cell assay.

RTCA software 2.0 (ACEA Biosciences, Inc.) was used to record all experimental data. Data were analyzed using GraphPad Prism 8.0. Compound responses, baseline-corrected to vehicle control, were normalized at the time of ligand addition to obtain Normalized Cell Index (NCI) values to correct for compound-independent responses. The time of normalization was either at approximately 19 hr 30 min, at 23 hr 30 min or at 24 hr after cell seeding for analysis of NECA response depending on the type of assay (number of steps), *i.e.* pre-treatment with antagonists, washing and NECA treatment, respectively.

The absolute values of Area Under the Curve (AUC) up to 90 min after NECA addition were exported to Graphpad Prism for further analysis yielding concentration–response curves. The pEC_{50} value of NECA (Table 5) was obtained using non-linear regression curve fitting of AUC data into "log(agonist) vs. response (three parameters)" analysis. pIC_{50} values of hA_{2B}AR antagonists (Table 5) were obtained using non-linear regression curve fitting of AUC data into "log(inhibitor) vs. response (three parameters)" analysis. Data shown are the mean ± SEM of at least three

individual experiments performed in duplicate.

References

1. Jacobson, M. A.; Johnson, R. G.; Luneau, C. J.; Salvatore, C. A. Cloning and Chromosomal Localization of the Human A2b Adenosine Receptor Gene (ADORA2B) and Its Pseudogene. *Genomics* 1995, 27, 374-376.
2. Fredholm, B. B.; IJzerman, A. P.; Jacobson, K. A.; Klotz, K.-N.; Linden, J. International Union of Pharmacology. XXV. Nomenclature and Classification of Adenosine Receptors. *Pharmacological Reviews* 2001, 53, 527-552.
3. Gessi, S.; Varani, K.; Merighi, S.; Leung, E.; Mac Lennan, S.; Baraldi, P. G.; Borea, P. A. Novel selective antagonist radioligands for the pharmacological study of A2B adenosine receptors. *Purinergic Signalling* 2006, 2, 583-588.
4. Beukers, M. W.; den Dulk, H.; van Tilburg, E. W.; Brouwer, J.; IJzerman, A. P. Why Are A_{2B} Receptors Low-Affinity Adenosine Receptors? Mutation of Asn273 to Tyr Increases Affinity of Human A_{2B} Receptor for 2-(1-Hexynyl)adenosine. *Molecular Pharmacology* 2000, 58, 1349-1356.
5. Fredholm, B. B.; IJzerman, A. P.; Jacobson, K. A.; Linden, J.; Muller, C. E. International Union of Basic and Clinical Pharmacology. LXXXI. Nomenclature and classification of adenosine receptors--an update. *Pharmacol Rev* 2011, 63, 1-34.
6. Feoktistov, I.; Biaggioni, I. Adenosine A2B receptors. *Pharmacol Rev* 1997, 49, 381-402.
7. Zhou, Y.; Schneider, D. J.; Blackburn, M. R. Adenosine signaling and the regulation of chronic lung disease. *Pharmacol Ther* 2009, 123, 105-16.
8. Spicuzza, L.; Di Maria, G.; Polosa, R. Adenosine in the airways: implications and applications. *Eur J Pharmacol* 2006, 533, 77-88.
9. Kolachala, V. L.; Vijay-Kumar, M.; Dalmasso, G.; Yang, D.; Linden, J.; Wang, L.; Gewirtz, A.; Ravid, K.; Merlin, D.; Sitaraman, S. V. A2B adenosine receptor gene deletion attenuates murine colitis. *Gastroenterology* 2008, 135, 861-70.
10. El-Tayeb, A.; Michael, S.; Abdelrahman, A.; Behrenswerth, A.; Gollos, S.; Nieber, K.; Müller, C. E. Development of Polar Adenosine A2A Receptor Agonists for Inflammatory Bowel Disease: Synergism with A2B Antagonists. *ACS Medicinal Chemistry Letters* 2011, 2, 890-895.
11. Harada, H.; Asano, O.; Hoshino, Y.; Yoshikawa, S.; Matsukura, M.; Kabasawa, Y.; Niijima, J.; Kotake, Y.; Watanabe, N.; Kawata, T.; Inoue, T.; Horizoe, T.; Yasuda, N.; Minami, H.; Nagata, K.; Murakami, M.; Nagaoka, J.; Kobayashi, S.; Tanaka, I.; Abe, S. 2-Alkynyl-8-aryl-9-methyladenines as novel adenosine receptor antagonists: their synthesis and structure-activity relationships toward hepatic glucose production induced via agonism of the A(2B) receptor. *J Med Chem* 2001, 44, 170-9.
12. Wei, Q.; Costanzi, S.; Balasubramanian, R.; Gao, Z. G.; Jacobson, K. A. A2B

adenosine receptor blockade inhibits growth of prostate cancer cells. *Purinergic Signal* 2013, 9, 271-80.

13. Vigano, S.; Alatzoglou, D.; Irving, M.; Menetrier-Caux, C.; Caux, C.; Romero, P.; Coukos, G. Targeting Adenosine in Cancer Immunotherapy to Enhance T-Cell Function. *Front Immunol* 2019, 10, 925.
14. Gao, Z.-G.; Jacobson, K. A. A_{2B} Adenosine Receptor and Cancer. *Int. J. Mol. Sci.* 2019, 20, 5139.
15. Kalla, R. V.; Zablocki, J. Progress in the discovery of selective, high affinity A(2B) adenosine receptor antagonists as clinical candidates. *Purinergic signalling* 2009, 5, 21-29.
16. Müller, C. E.; Baqi, Y.; Hinz, S.; Namasivayam, V. Medicinal Chemistry of A2B Adenosine Receptors. In *The Adenosine Receptors*, Borea, P. A.; Varani, K.; Gessi, S.; Merighi, S.; Vincenzi, F., Eds. Springer International Publishing: Cham, 2018; pp 137-168.
17. Clinical Trials. PBF-1129 in Patients With NSCLC. (Accessed on 13-Nov-2019, https://clinicaltrials.gov/ct2/show/NCT03274479?term=ADORA2B&draw=2&rank=1).
18. Sherbiny, F. F.; Schiedel, A. C.; Maass, A.; Muller, C. E. Homology modelling of the human adenosine A2B receptor based on X-ray structures of bovine rhodopsin, the beta2-adrenergic receptor and the human adenosine A2A receptor. *Journal of computer-aided molecular design* 2009, 23, 807-28.
19. Swinney, D. C.; Haubrich, B. A.; Van Liefde, I.; Vauquelin, G. The Role of Binding Kinetics in GPCR Drug Discovery. *Curr Top Med Chem* 2015, 15, 2504-22.
20. Lindström, E.; von Mentzer, B.; Påhlman, I.; Ahlstedt, I.; Uvebrant, A.; Kristensson, E.; Martinsson, R.; Novén, A.; de Verdier, J.; Vauquelin, G. Neurokinin 1 Receptor Antagonists: Correlation between in Vitro Receptor Interaction and in Vivo Efficacy. *Journal of Pharmacology and Experimental Therapeutics* 2007, 322, 1286-1293.
21. Kim, Y.-C.; Ji, X.-d.; Melman, N.; Linden, J.; Jacobson, K. A. Anilide Derivatives of an 8-Phenylxanthine Carboxylic Congener Are Highly Potent and Selective Antagonists at Human A2B Adenosine Receptors. *Journal of Medicinal Chemistry* 2000, 43, 1165-1172.
22. Borrmann, T.; Hinz, S.; Bertarelli, D. C. G.; Li, W.; Florin, N. C.; Scheiff, A. B.; Müller, C. E. 1-Alkyl-8-(piperazine-1-sulfonyl)phenylxanthines: Development and Characterization of Adenosine A2B Receptor Antagonists and a New Radioligand with Subnanomolar Affinity and Subtype Specificity. *Journal of Medicinal Chemistry* 2009, 52, 3994-4006.
23. Motulsky, H. J.; Mahan, L. C. The kinetics of competitive radioligand binding predicted by the law of mass action. *Mol Pharmacol* 1984, 25, 1-9.
24. Sykes, D. A.; Stoddart, L. A.; Kilpatrick, L. E.; Hill, S. J. Binding kinetics of ligands acting at GPCRs. *Molecular and Cellular Endocrinology* 2019, 485, 9-19.
25. Guo, D.; Hillger, J. M.; IJzerman, A. P.; Heitman, L. H. Drug-Target Residence Time—A Case for G Protein-Coupled Receptors. *Medicinal Research Reviews*

2014, 34, 856-892.

26. Bradshaw, J. M.; McFarland, J. M.; Paavilainen, V. O.; Bisconte, A.; Tam, D.; Phan, V. T.; Romanov, S.; Finkle, D.; Shu, J.; Patel, V.; Ton, T.; Li, X.; Loughhead, D. G.; Nunn, P. A.; Karr, D. E.; Gerritsen, M. E.; Funk, J. O.; Owens, T. D.; Verner, E.; Brameld, K. A.; Hill, R. J.; Goldstein, D. M.; Taunton, J. Prolonged and tunable residence time using reversible covalent kinase inhibitors. *Nature chemical biology* 2015, 11, 525-31.
27. Tsuruda, P. R.; Yung, J.; Martin, W. J.; Chang, R.; Mai, N.; Smith, J. A. Influence of ligand binding kinetics on functional inhibition of human recombinant serotonin and norepinephrine transporters. *Journal of pharmacological and toxicological methods* 2010, 61, 192-204.
28. Vlachodimou, A.; Konstantinopoulou, K.; IJzerman, A. P.; Heitman, L. H. Affinity, binding kinetics and functional characterization of draflazine analogues for human equilibrative nucleoside transporter 1 (SLC29A1). *Biochemical Pharmacology* 2020, 172, 113747.
29. Costa, B.; Da Pozzo, E.; Giacomelli, C.; Barresi, E.; Taliani, S.; Da Settimo, F.; Martini, C. TSPO ligand residence time: a new parameter to predict compound neurosteroidogenic efficacy. *Scientific Reports* 2016, 6, 18164.
30. de Witte, W. E. A.; Danhof, M.; van der Graaf, P. H.; de Lange, E. C. M. In vivo Target Residence Time and Kinetic Selectivity: The Association Rate Constant as Determinant. *Trends in pharmacological sciences* 2016, 37, 831-842.
31. Tonge, P. J. Drug-Target Kinetics in Drug Discovery. *ACS chemical neuroscience* 2017, 9, 29-39.
32. Smith, G. F. Medicinal Chemistry by the Numbers: The Physicochemistry, Thermodynamics and Kinetics of Modern Drug Design. In *Progress in Medicinal Chemistry*, Lawton, G.; Witty, D. R., Eds. Elsevier: 2009; Vol. 48, pp 1-29.
33. IJzerman, A. P.; Guo, D. Drug–Target Association Kinetics in Drug Discovery. *Trends in Biochemical Sciences* 2019, 44, 861-871.
34. Tummino, P. J.; Copeland, R. A. Residence Time of Receptor−Ligand Complexes and Its Effect on Biological Function. *Biochemistry* 2008, 47, 5481-5492.
35. Copeland, R. A. The drug-target residence time model: a 10-year retrospective. *Nat Rev Drug Discov* 2016, 15, 87-95.
36. Tonge, P. J. Drug-Target Kinetics in Drug Discovery. *ACS chemical neuroscience* 2018, 9, 29-39.
37. Zablocki, J.; Elzein, E.; Kalla, R. A2B adenosine receptor antagonists and their potential indications. *Expert Opinion on Therapeutic Patents* 2006, 16, 1347-1357.
38. Ji, X.; Kim, Y. C.; Ahern, D. G.; Linden, J.; Jacobson, K. A. [3H]MRS 1754, a selective antagonist radioligand for A(2B) adenosine receptors. *Biochemical pharmacology* 2001, 61, 657-663.
39. Xi, B.; Yu, N.; Wang, X.; Xu, X.; Abassi, Y. A. The application of cell-based label-free technology in drug discovery. *Biotechnology journal* 2008, 3, 484-95.

40. Yu, N.; Atienza, J. M.; Bernard, J.; Blanc, S.; Zhu, J.; Wang, X.; Xu, X.; Abassi, Y. A. Real-Time Monitoring of Morphological Changes in Living Cells by Electronic Cell Sensor Arrays: An Approach To Study G Protein-Coupled Receptors. *Analytical Chemistry* 2006, 78, 35-43.

41. Fang, Y. The development of label-free cellular assays for drug discovery. *Expert Opinion on Drug Discovery* 2011, 6, 1285-1298.

42. de Zwart, M.; Link, R.; von Frijtag Drabbe Kunzel, J. K.; Cristalli, G.; Jacobson, K. A.; Townsend-Nicholson, A.; IJzerman, A. P. A functional screening of adenosine analogues at the adenosine A2B receptor: a search for potent agonists. *Nucleosides & nucleotides* 1998, 17, 969-85.

43. de Lera Ruiz, M.; Lim, Y.-H.; Zheng, J. Adenosine A2A Receptor as a Drug Discovery Target. *Journal of Medicinal Chemistry* 2014, 57, 3623-3650.

44. Beattie, D.; Brearley, A.; Brown, Z.; Charlton, S. J.; Cox, B.; Fairhurst, R. A.; Fozard, J. R.; Gedeck, P.; Kirkham, P.; Meja, K.; Nanson, L.; Neef, J.; Oakman, H.; Spooner, G.; Taylor, R. J.; Turner, R. J.; West, R.; Woodward, H. Synthesis and evaluation of two series of 4′-aza-carbocyclic nucleosides as adenosine A2A receptor agonists. *Bioorganic & Medicinal Chemistry Letters* 2010, 20, 1219-1224.

45. Aurelio, L.; Baltos, J.-A.; Ford, L.; Nguyen, A. T. N.; Jörg, M.; Devine, S. M.; Valant, C.; White, P. J.; Christopoulos, A.; May, L. T.; Scammells, P. J. A Structure–Activity Relationship Study of Bitopic N6-Substituted Adenosine Derivatives as Biased Adenosine A1 Receptor Agonists. *Journal of Medicinal Chemistry* 2018, 61, 2087-2103.

46. Devine, S. M.; May, L. T.; Scammells, P. J. Design, synthesis and evaluation of N6-substituted 2-aminoadenosine-5′-N-methylcarboxamides as A3 adenosine receptor agonists. *MedChemComm* 2014, 5, 192-196.

47. Schulte, G.; Fredholm, B. B. Human adenosine A(1), A(2A), A(2B), and A(3) receptors expressed in Chinese hamster ovary cells all mediate the phosphorylation of extracellular-regulated kinase 1/2. *Mol Pharmacol* 2000, 58, 477-82.

48. Doornbos, M. L. J.; Cid, J. M.; Haubrich, J.; Nunes, A.; van de Sande, J. W.; Vermond, S. C.; Mulder-Krieger, T.; Trabanco, A. A.; Ahnaou, A.; Drinkenburg, W. H.; Lavreysen, H.; Heitman, L. H.; IJzerman, A. P.; Tresadern, G. Discovery and Kinetic Profiling of 7-Aryl-1,2,4-triazolo[4,3-a]pyridines: Positive Allosteric Modulators of the Metabotropic Glutamate Receptor 2. *J Med Chem* 2017, 60, 6704-6720.

49. Jacobson, K. A.; Kirk, K. L.; Padgett, W. L.; Daly, J. W. Functionalized congeners of 1,3-dialkylxanthines: preparation of analogs with high affinity for adenosine receptors. *Journal of Medicinal Chemistry* 1985, 28, 1334-1340.

50. Smith, P. K.; Krohn, R. I.; Hermanson, G. T.; Mallia, A. K.; Gartner, F. H.; Provenzano, M. D.; Fujimoto, E. K.; Goeke, N. M.; Olson, B. J.; Klenk, D. C. Measurement of protein using bicinchoninic acid. *Analytical biochemistry* 1985, 150, 76-85.

51. Hillger, J. M.; Schoop, J.; Boomsma, D. I.; Eline Slagboom, P.; IJzerman, A. P.; Heitman, L. H. Whole-cell biosensor for label-free detection of GPCR-mediated drug responses in personal cell lines. *Biosensors and Bioelectronics* 2015, 74, 233-242.

52. Cheng, Y.; Prusoff, W. H. Relationship between the inhibition constant (KI) and the concentration of inhibitor which causes 50 per cent inhibition (I50) of an enzymatic reaction. *Biochemical Pharmacology* 1973, 22, 3099-3108.

53. Copeland, R. A. Evaluation of enzyme inhibitors in drug discovery. A guide for medicinal chemists and pharmacologists. *Methods Biochem Anal* 2005, 46, 1-265.